Available online at www.sciencedirect.com
ScienceDirect
Journal of the European Ceramic Society 32 (2012) 49–57
www.elsevier.com/locate/jeurceramsoc

Developments on the mechanical properties of $MgO–MgAl_2O_4$ composite refractories by $ZrSiO_4$–3 mol% Y_2O_3 addition

Baris Sahin, Cemail Aksel *

Department of Materials Science and Engineering, Anadolu University, Iki Eylul Campus, Eskisehir 26470, Turkey

Received 1 July 2011; received in revised form 15 July 2011; accepted 23 July 2011
Available online 25 August 2011

Abstract

Improvements and the effects of additions of $ZrSiO_4$–3 mol% Y_2O_3 into $MgO–MgAl_2O_4$ composite refractories on mechanical properties and thermal stress resistance parameters were investigated. Significant improvements were achieved on mechanical properties and $R–R_{st}$ parameters up to ~2 and ~3-fold ratios. The major parameters improving mechanical properties and thermal behaviour of refractories were determined as follows: (i) the increase in resistance to crack initiation and propagation due to formation of Mg_2SiO_4 phase after decomposition of zircon; (ii) propagation of the microcracks formed in the structure for a short distance by interlinking each other; (iii) arresting or deviation of microcracks when reaching pores or ZrO_2 grains released after dissociation of zircon, located together with Y_2O_3 particles, and furthermore; (iv) co-presence of both intergranular and transgranular types of cracks, and with incorporation of zircon–Y_2O_3; (v) increase in density; and (vi) a significant reduction in MgO grain size.

Keywords: MgO; Spinel; Zircon; Y_2O_3; Refractories; Mechanical properties

1. Introduction

Magnesium aluminate spinel ($MgAl_2O_4$) is obtained by reaction of mixtures of MgO and Al_2O_3. Theoretically, the stoichiometric composition of $MgAl_2O_4$ contains 71.68% Al_2O_3 and 28.32% MgO by weight. MgO is one of the most important inputs of the refractory materials industry due to its high melting point. Although MgO–chrome refractories and MgO and dolomite origin refractories are adequate in many aspects in terms of their fields of application, their resistance against thermal shock is low.[1,2] It was found that this shortcoming may be covered by producing MgO–spinel refractory materials with addition of $MgAl_2O_4$ spinel particles to the MgO matrix.[1,2] The fact that toxic Cr^{6+} ions produced from Cr_2O_3 have allergenic, ulcerogenic and carcinogenic effects on the skin in MgO–chrome refractories has been cause of concern, bringing out the need for use of alternative MgO–spinel refractories not containing chrome.[3] When chrome ore reacts with alkalis to form potassium chromate or potassium dichromate (containing Cr^{6+}), this can result in the destruction of the brick.[4,5] Hexavalent chromium diffuses from the refractory into the cement clinker, and increases the risk of toxic reactions during processing of the cement.[6] The most important factor in prevalent use of MgO–spinel refractories among other MgO and dolomite origin refractory materials is their having higher resistance against thermal shock and alkali attacks.[7] MgO–spinel materials have ~1.5–2 times longer useful lives compared to other basic bricks like MgO–chrome.[6]

The main advantages of using MgO–spinel bricks in cement kilns can also be summarised as follows[8–11]: (i) low thermal expansion coefficient of MgO–spinel bricks, (ii) high resistance to thermo-mechanical stress, (iii) chemical resistance to oil and ash deposits, (iv) high resistance to corrosion and changes in kiln atmosphere, (v) low content of secondary oxides, which results in minimal alteration in structure of the hot face in service, (vi) elimination of chromite, which makes the brick less susceptible to alkali attack in service, (vii) no toxic Cr^{6+} ions leached from waste materials, and (viii) white cements can be made without discoloration problems caused by transition metal cations.

As compared to MgO-based materials, MgO–spinel refractory materials display a higher resistance against thermal shocks. It is reported[12,13] that incorporation of (i) spinel into MgO

* Corresponding author. Tel.: +90 222 3350580x6362; fax: +90 222 3239501.
E-mail address: caksel@anadolu.edu.tr (C. Aksel).

0955-2219/$ – see front matter © 2011 Elsevier Ltd. All rights reserved.
doi:10.1016/j.jeurceramsoc.2011.07.024

Table 1
Compositions prepared for mechanical testing where weights of MgO (0–1 mm), spinel (0–1 mm), $ZrSiO_4$ (~13 μm) and 3 mol% Y_2O_3 (~4 μm) correlated with ZrO_2 content in $ZrSiO_4$ were used.

Compositions	MgO (%)	Spinel (%)	$ZrSiO_4$ (%)	Y_2O_3* (%)
M	100.00	–	–	–
M–5%S	95.00	5	–	–
M–10%S	90.00	10	–	–
M–20%S	80.00	20	–	–
M–30%S	70.00	30	–	–
M–30%S–20%zircon	50.00	30	20	–
M–5%S–5%(zircon + Y)	89.83	5	5	0.17
M–5%S–10%(zircon + Y)	84.66	5	10	0.34
M–5%S–20%(zircon + Y)	74.31	5	20	0.69
M–5%S–30%(zircon + Y)	63.97	5	30	1.03
M–10%S–5%(zircon + Y)	84.83	10	5	0.17
M–10%S–10%(zircon + Y)	79.66	10	10	0.34
M–10%S–20%(zircon + Y)	69.31	10	20	0.69
M–10%S–30%(zircon + Y)	58.97	10	30	1.03
M–20%S–5%(zircon + Y)	74.83	20	5	0.17
M–20%S–10%(zircon + Y)	69.66	20	10	0.34
M–20%S–20%(zircon + Y)	59.31	20	20	0.69
M–20%S–30%(zircon + Y)	48.97	20	30	1.03
M–30%S–5%(zircon + Y)	64.83	30	5	0.17
M–30%S–10%(zircon + Y)	59.66	30	10	0.34
M–30%S–20%(zircon + Y)	49.31	30	20	0.69
M–30%S–30%(zircon + Y)	38.97	30	30	1.03

* The amounts of 3 mol% Y_2O_3 equivalent to ZrO_2 proportion in zircon were calculated for each composition and subsequently those quantities of Y_2O_3 (Y) were converted to weight percentages.

significantly improves the retained strength after thermal shock, hot modulus of rupture, refractoriness under load and (ii) Y_2O_3 into MgO–spinel markedly develops densification and hot strength characteristics of MgO–spinel composite refractories. With the addition of spinel particles to MgO, the service life of composite refractory materials increase, specifically due to the increase in the work of fracture energy, while a decrease occurs in other mechanical properties.[14–17] This study was carried out for achieving improvement on the mechanical properties of materials obtained by incorporating varied amounts of zircon and 3 mol% Y_2O_3 into MgO–spinel composite refractories containing varied ratios of spinel ($MgAl_2O_4$), increasing their resistance especially against fracture, obtaining high thermo-mechanical properties through analysis of R and R_{st} thermal stress/shock parameters data and hence increasing their further service life. In this study, the relationships between the mechanisms causing improvement on the mechanical properties of composite refractories and microstructural changes and parameters affecting these were investigated in detail and explained with reasons, aiming to make this work a useful step for industrial applications.

2. Experimental

As shown in Table 1, recipes were prepared by adding weights of 5%, 10%, 20% and 30% zircon ($ZrSiO_4$) and 3 mol% Y_2O_3 (Y) correlated with ZrO_2 content in zircon to compositions obtained by additions of 5%, 10%, 20% and 30% $MgAl_2O_4$ spinel (S) by weight to MgO (M). The amounts of 3 mol% Y_2O_3 equivalent to ZrO_2 proportion in zircon were calculated for each composition, where those quantities of Y_2O_3 were subsequently converted to weight percentages, and given in Table 1. Batches prepared using MgO (0–1 mm), spinel (0–1 mm), zircon (~13 μm) and Y_2O_3 (~4 μm) were shaped into samples of $\sim 8 \times 8 \times 60\,mm^3$ under a pressure of ~100 MPa. The samples were sintered for 2 h in kiln (Nabertherm HT16/18) at 1600 °C using heating and cooling rates of 5 °C/min. Bulk density and apparent porosity values of 3 specimens from each composition were measured using the standard water immersion method and average values were taken.[18] After samples were ground using 800 and 1200 grade SiC papers until obtaining smooth surfaces based on the standard sample preparation rules,[15,19] the samples were dehydrated at ~110 °C in an oven and mechanical tests were carried out. The mechanical tests performed using a load cell of 2 kN moving at a velocity of 0.5 mm/min with support roller span (L) of 40 mm were applied to minimum 5–6 samples and average values were taken. Under standard tests; values of strength[19] (σ), modulus of elasticity[20] $\{E = L^3m/(4WD^3)\}$, fracture toughness[21–24] $\{K_{1C} = (3/2)(PLc^{1/2}Y)/(WD^2)\}$, fracture surface energy, γ_S,[25] $\{K_{1C} = (2E\gamma_S)^{1/2}\}$ and work of fracture energy[26] $\{\gamma_{WOF} = U/[2W(D-c)]\}$ were determined by the 3-point bending method in Instron 5581. K_{1C}, γ_S and γ_{WOF} measurements were carried out using single edge notched beam (SENB) method. The parameters used in those equations given above are as follows[19–26]: m is slope of the tangent of the initial straight-line portion of the load-deflection curve, W is the specimen width, D is the specimen thickness, P is the load at failure, c is the notch depth, and Y is a dimensionless constant that depends on the geometry of the loading and the crack configuration. Y values for all compositions were determined depending

Table 2
Mechanical properties and densities of composite refractories having M, M–30%S, M–30%S–20%zircon and M–30%S–20%(zircon + Y) compositions.

	MgO	M–30%S	M–30%S–20%zircon	M–30%S–20%(zircon + Y)
σ (MPa)	48.51 ± 5.50	11.32 ± 0.54	20.69 ± 2.05	21.25 ± 3.96
E (GPa)	35.07 ± 2.37	7.88 ± 0.87	13.82 ± 1.36	15.20 ± 2.87
K_{1C} (MPa.m$^{1/2}$)	1.52 ± 0.08	0.51 ± 0.04	0.81 ± 0.01	1.09 ± 0.11
γ_S (J/m^2)	32.81 ± 3.65	16.40 ± 2.60	24.20 ± 5.09	39.02 ± 7.65
γ_{WOF} (J/m^2)	27.43 ± 3.09	67.62 ± 6.16	61.29 ± 11.81	59.76 ± 1.53
ρ (g/cm^3)	2.80 ± 0.03	2.79 ± 0.01	3.04 ± 0.04	3.20 ± 0.05

on the specimen dimensions and represented by fourth-degree polynomials of the following form to within 0.2% for all values of c/D up to 0.6, where the coefficients A had the subsequent values: $\{Y = A_0 + A_1(c/D) + A_2(c/D)^2 + A_3(c/D)^3 + A_4(c/D)^4\}$, for $L/D \sim 8$, $A_0 = 1.96$, $A_1 = -2.75$, $A_2 = 13.66$, $A_3 = -23.98$ and $A_4 = 25.22$.[21–24] The magnitude of critical defect size (C) value was calculated using Griffith equation[25,27–30] $\{\sigma = (2E\gamma_S/\pi C)^{1/2}\}$,[19,21–25,27–30] where combining the SENB fracture surface energy values with those of strength allowed an estimate to be made of the critical defect size.[15,31] E values were calculated using the slope of stress–strain curve in the initial linear portion of the curve between lower and upper bounds by reporting the steepest slope as the modulus, where the correction for machine stiffness was also considered as follow: after loading the machine with load cell against itself without any specimen using a very low crosshead speed, the slope of this displacement measured for a given load was being subtracted from the slope of specimen's stress–strain curve.[32,33] Work of fracture is usually interpreted as the work done in propagating a crack to break a notched specimen, divided by twice the fracture surface areas (since two new faces are created). γ_{WOF}[26] is the amount of energy required to propagate a crack completely through a specimen, which is calculated by determining the area remaining under the load–deflection curve (U). K_{1C}, γ_S and γ_{WOF} values were calculated by using notches at a depth of ~25% of thickness (~2 mm) of the material using a diamond disk 700 μm thick on specimens. Notch depth was measured using an Olympus BX60M brand optical microscope. X-ray diffraction (XRD) analysis was performed using Rigaku RINT2000 equipment. SEM studies were carried out using Zeis Evo 50 device with the microstructures and fracture surfaces of materials analyzed. Using photographs taken on the surfaces of specimens, which were polished and thermally etched for 10 min at 1450 °C, the average MgO grain size was calculated using a standard line mean intercept method[34] ($D = 1.56L$, D: the average grain size, L: the average intercept length). Hasselman parameters, which determine the fracture resistance of materials due to thermal stress/shock and used in estimation of maximum thermal resistance, were calculated by following formulas[35]: $\{R = [\sigma.(1-\nu)]/(E.\alpha)\}$ and $\{R_{st} = [\gamma_S/(\alpha^2.E)]^{1/2}\}$, where α is the mean thermal expansion coefficient of the composite refractory and ν is the Poisson's ratio. In this study, (i) mechanical properties and (ii) values of R and R_{st} thermal stress/shock parameters determining high temperature performance of composite refractory materials were determined and the relationships between obtained data and microstructural changes were analyzed in detail, with the parameters affecting these examined.

3. Results and discussion

Results of mechanical tests on composites refractories produced by adding varied amounts of $ZrSiO_4$ + 3 mol% Y_2O_3(zircon + Y) to MgO–spinel (M–S) materials containing varied ratios of spinel ($MgAl_2O_4$) are given below. The additives used in figures and tables represent: (i) $MgAl_2O_4$ for M–S and (ii) $ZrSiO_4 + Y_2O_3$ for M–S–(zircon + Y) materials. As shown in Table 2, mechanical tests were initially carried out for the following materials where their compositions were given in Table 1: (i) MgO (M), (ii) M–30%S, (iii) M–30%S–20% zircon composition selected as a model without addition of Y_2O_3 (Y) and (iv) M–30%S–20%(zircon + Y) composition in terms of observing the effects of Y_2O_3 addition and improvements on mechanical properties, and their results were evaluated in comparison with each other.

Generally, a marked increase was observed in the mechanical properties of M–S–(zircon + Y) composite refractories compared to M–S containing no additives. With the addition of 20%zircon to M–30%S, as illustrated in Table 2, a 1.8-fold increase was observed in strength (σ), 1.8-fold in modulus of elasticity (E), 1.6-fold in fracture toughness (K_{1C}) and 1.5-fold in fracture surface energy (γ_S). The improvements observed in the composition obtained by adding 20%(zircon + Y) to M–30%S were 1.9-fold in both strength and modulus of elasticity, 2.1-fold in fracture toughness and 2.4-fold in fracture surface energy (Table 2). Work of fracture energy (γ_{WOF}) data show a significant increase with incorporation of additives into MgO and in general those values are close to each other. Zircon and zircon + Y additives incorporated into M–S have significantly increased the density values of the new compositions obtained. Comparing M–30%S–20%zircon and M–30%S–20%(zircon + Y) compositions, it was determined that the addition of Y_2O_3 has lead to improvements in specifically the values of fracture toughness and fracture surface energy by factors of 34.6% and 61.2%, respectively (Table 2).

In general; the addition of 20%(zircon + Y) to M–30%S has increased the mechanical properties significantly when compared to M–30%S–20%zircon to which only zircon was added. Therefore, mechanical tests were performed by adding varied ratios of zircon + Y to M–S materials in the subsequent parts of the performed study where all the compositions were given

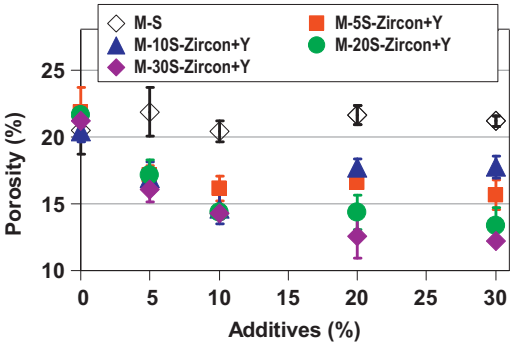

Fig. 1. Open porosity as a function of additives {additives: (i) $MgAl_2O_4$ for M–S and (ii) $ZrSiO_4 + Y_2O_3$ for M–S–(zircon + Y)}.

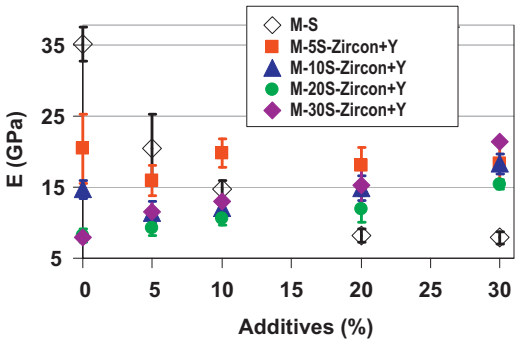

Fig. 3. Modulus of elasticity (E) as a function of additives {additives: (i) $MgAl_2O_4$ for M–S and (ii) $ZrSiO_4 + Y_2O_3$ for M–S–(zircon + Y)}.

in Table 1. Optimum compositions were determined in terms of improving mechanical properties and the basic parameters affecting development were investigated. It was also aimed to increase the thermal shock performance and hence prolong the service life of these composite refractories used at high temperatures by calculation of the thermal stress/shock parameters.

Density (ρ) and open porosity results are given in Table 2 and Fig. 1, respectively. As shown in Table 2, density values increase significantly with the addition of additives[36,37] (ρ_{zircon}: 4.56 g/cm^3, $\rho_{Y_2O_3}$: 5.046 g/cm^3), which have higher densities compared to M–S (ρ_{M-S}: 3.58 g/cm^3). On the contrary, the open porosity values of M–S–(zircon + Y) containing composite refractories are lower than those of M–S materials and decrease significantly when the amount of additive is increased (Fig. 1). The density values of M–S–(zircon + Y) samples rise continuously with increasing amounts of additives. It was determined that the effect of use of zircon + Y on density and open porosity is much higher than for spinel. The highest density and the lowest open porosity values were attained in M–30%S–30%(zircon + Y) composition. The average density values measured for M and M–S composite refractories were ~2.8 g/cm^3, rising up to ~3.3 g/cm^3 with increased amounts of added zircon + Y. Porosity is ~21% in M and M–S materials, displaying a downwards trend reaching ~12% with the increase in the amount of zircon + Y added to M–S.

As shown in Fig. 2, it was observed that the strength (σ) values of composite refractories to which more than 5% zircon + Y was added are higher than the strength values of M–S materials with no additive. The highest strength value was attained in M–30%S–30%(zircon + Y) composition with an increase of 2.9-fold observed in the strength value compared to M–30%S containing no additives. The modulus of elasticity (E) values of M–S–(zircon + Y) composite refractories in general increase with increased amount of additives. With incorporation of ≥10% additive, the modulus of elasticity values have displayed a marked increase in M–S–(zircon + Y) compositions compared to M–S materials (Fig. 3). A 2.7-fold improvement was observed in the modulus of elasticity when 30%(zircon + Y) was added to M–30%S material.

The fracture toughness (K_{1c}) values of composite refractories obtained by incorporating varied ratios of ≥10%(zircon + Y) into M–S are in general higher than K_{1c} values of additive free M–S materials (Fig. 4). For example, in K_{1c} values obtained as a result of addition of 20% and 30% zircon + Y to M–30%S, improvements of 2.1-fold and 2.4-fold were observed respectively compared to M–30%S. The fracture surface energy (γ_S) values of M–S–(zircon + Y) composite refractories are higher than the γ_S values of additive free M–S materials when ≥10% (zircon + Y) is added into M–S. Similarly; in the γ_S values obtained by adding 20% and 30% zircon + Y to M–30%S–(zircon + Y) composition, 2.4-fold and 2.0-fold improvements were observed respectively compared to M–30%S (Fig. 5).

The average MgO crystal size was calculated for different compositions selected as follows: (i) pure MgO = 67.2 μm, (ii) M–30%S = 31.2 μm and (iii)

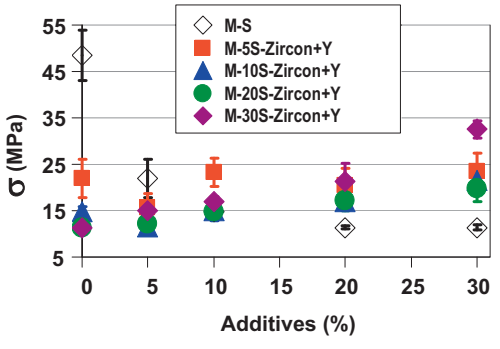

Fig. 2. Strength (σ) as a function of additives {additives: (i) $MgAl_2O_4$ for M–S and (ii) $ZrSiO_4 + Y_2O_3$ for M–S–(zircon + Y)}.

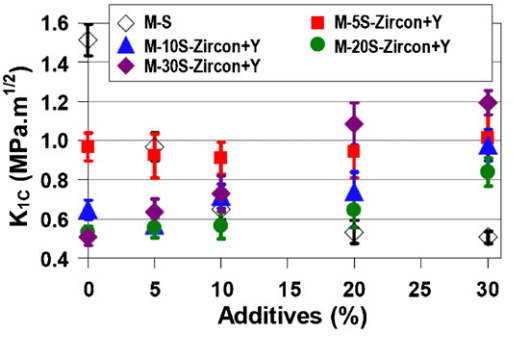

Fig. 4. Fracture toughness (K_{1C}) as a function of additives {additives: (i) $MgAl_2O_4$ for M–S and (ii) $ZrSiO_4 + Y_2O_3$ for M–S–(zircon + Y)}.

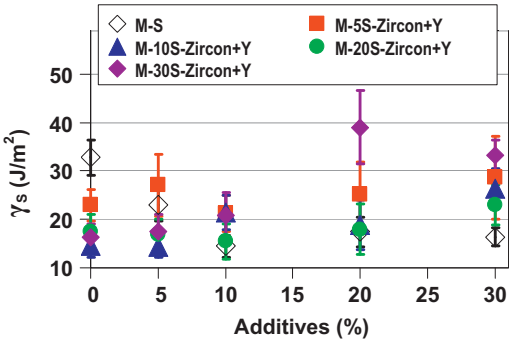

Fig. 5. Fracture surface energy (γ_S) as a function of additives {additives: (i) $MgAl_2O_4$ for M–S and (ii) $ZrSiO_4 + Y_2O_3$ for M–S–(zircon + Y)}.

M–30%S–20%(zircon + Y) = 25.3 μm. It was observed that there was a significant reduction in mean MgO grain size as the amount of additives was increased. Critical defect size (C) values as a function of additives are given in Fig. 6. It was observed from the analysis of all compositions with 5% additive, M–S–(zircon + Y) composites have C values approximately equivalent to or higher than those of M–S materials. For example, a 1.8-fold rise was achieved in C value with the addition of 5%(zircon + Y) to M–5%S composition (Fig. 6). For M–S compositions containing ≥10%(zircon + Y), even though the majority of M–S–(zircon + Y) compositions had lower C values than those of M–S materials, some part of them were found to be equivalent to or higher than the critical defect size of M–S composite refractories. In general; a significant increase was observed in the C values of all M–S and M–S–(zircon + Y) compositions into which additives were incorporated, compared to the additive free MgO. This increase observed in C values, where additives were incorporated into MgO, was also consistent with the marked decrease occurring in the grain size of MgO as the amount of additive was increased. These variations in critical defect size and MgO grain size are associated with the improvement in mechanical properties developed by means of toughening mechanisms.

Work of fracture energy (γ_{WOF}) values as a function of additives are given in Fig. 7. Comparing the γ_{WOF} values of M–S–(zircon + Y) composites with M–S materials, all compositions with 5% additive have approximately the same γ_{WOF} values. In the other additive proportions, on the other hand, the

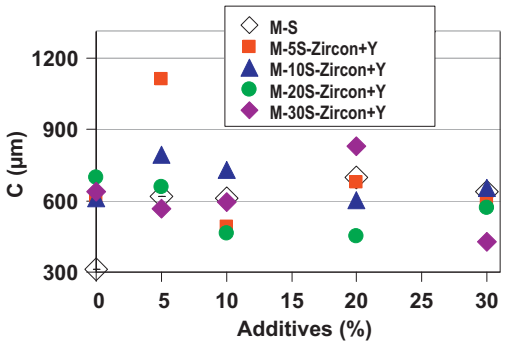

Fig. 6. Critical defect size (C) as a function of additives {additives: (i) $MgAl_2O_4$ for M–S and (ii) $ZrSiO_4 + Y_2O_3$ for M–S–(zircon + Y)}.

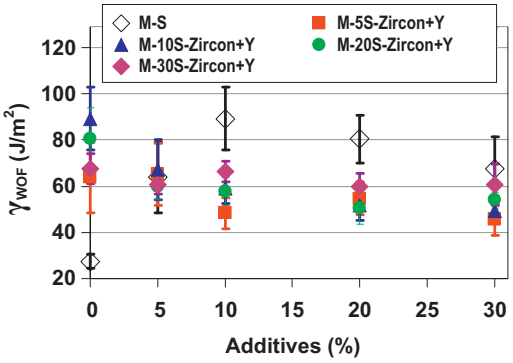

Fig. 7. Work of fracture energy (γ_{WOF}) as a function of additives {additives: (i) $MgAl_2O_4$ for M–S and (ii) $ZrSiO_4 + Y_2O_3$ for M–S–(zircon + Y)}.

γ_{WOF} values of M–S–(zircon + Y) composites are lower than the γ_{WOF} values of M–S materials. In general, the γ_{WOF} values are significantly higher than those of additive free MgO in the entirety of compositions containing M–S and M–S–(zircon + Y) as additives. The highest γ_{WOF} values among M–S–(zircon + Y) materials were achieved in M–30%S–(zircon + Y) compositions. γ_{WOF} values closest to those of M–S materials were obtained in M–30%S–(zircon + Y) composites compared to other M–S–(zircon + Y) compositions.

The fracture surface image of the composite refractory material produced with the addition of 20%(zircon + Y) to M–30%S is given in Fig. 8. The analysis of the fracture surfaces of M and M–S materials shows that there are mainly (i) transgranular cracks in MgO and (ii) intergranular cracks in M–S materials.[14,15,33] When zircon + Y was added to M–S on the other hand, it was observed that the intergranular and transgranular types of cracks occurred simultaneously (Fig. 8).

Fig. 9 shows schematic diagrams of load–deflection curves, for MgO and M–S–(zircon + Y) composite refractories. For additive free MgO, mostly transgranular cracks occurred and thus catastrophic failure occurred during fracture (Fig. 9a). The fracture of M–S materials containing zircon + Y is either primarily stable or rarely semi-stable, but never catastrophic

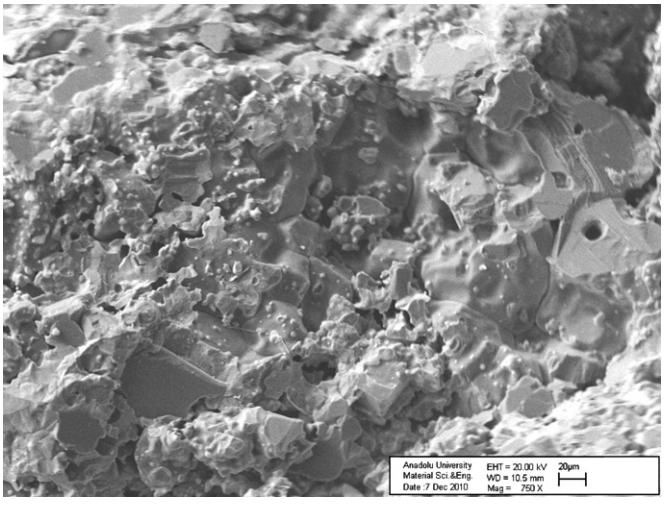

Fig. 8. Fracture surface image of a material with composition of M–30%S–20%(zircon + Y).

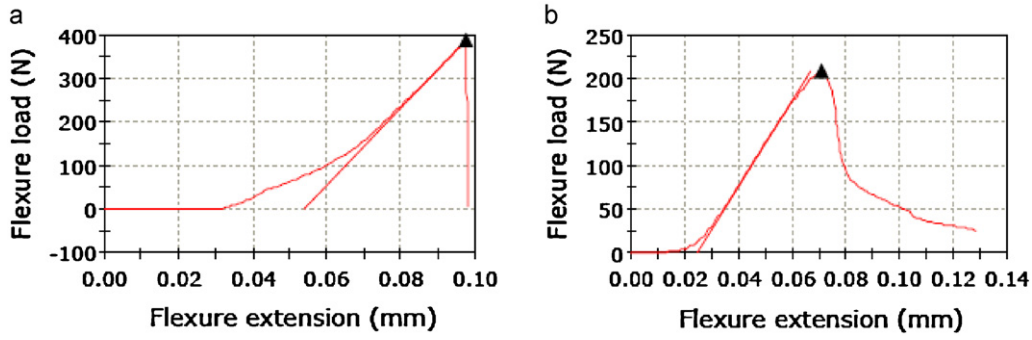

Fig. 9. Load–deflection curves for centred notched, 3-point bending specimens: (a) MgO (catastrophic) and (b) M–30%S–20%(zircon + Y) (stable).

(Fig. 9b). This is because the cracks were observed to travel around the smaller grains, propagating both intergranularly and transgranularly (Fig. 8). It therefore appears that higher values of mechanical properties (i.e. especially in K_{1C}, γ_S and γ_{WOF} values) are also associated with the occurrence of both intergranular and transgranular types of cracks with increasing amounts of zircon + Y in M–S compositions. The change in the fracture path of M–S–(zircon + Y) composite refractories resulted in an increase in the areas under the load–displacement curve, which indicated significant microcrack extension and interlinking with the higher K_{1C}, γ_S and γ_{WOF} values, requiring more energy for the fracture process and thus those materials showed stable crack growth (non-catastrophic failure).

The results of X-ray diffraction (XRD) analysis for M–30%S–20%(zircon + Y) composition selected as an example sample showing significant improvements on mechanical properties are given in Fig. 10. According to the phase analysis results; forsterite ($2MgO.SiO_2$) and cubic zirconia phases were identified besides MgO and spinel phases, in M–S–(zircon + Y) composite refractories analyzed. Furthermore, when microstructure and the distribution of elements were examined for M–30%S–20%(zircon + Y) composite refractory, it was observed that MgO and SiO_2 distributions were generally located in the similar regions and that forsterite (Mg_2SiO_4) phase was formed with the aid of also microstructural analyses (Fig. 11). A stronger bond is formed between the additives and the grains of main constituent due to the formation of the forsterite phase as a result of the reaction between SiO_2, which is

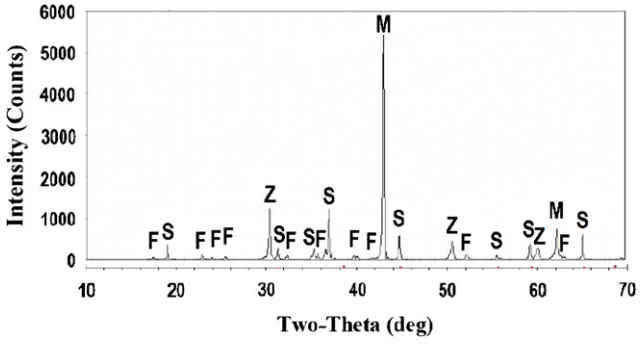

Fig. 10. XRD graph of a composite refractory having M–30%S–20%(zircon + Y) composition (M: MgO, Z: ZrO_2, F: Mg_2SiO_4, S: $MgAl_2O_4$).

released after decomposition of zircon as ZrO_2 and SiO_2 during sintering, and MgO that is the main phase. It was determined that sintering was more effective with the formation of the new phase. This is consistent with the rise in density values and the drop in the amount of porosity occurring due to the increase in the quantity of zircon + Y incorporated into M–S materials.

As shown in microstructures in Figs. 11 and 12, the white coloured ZrO_2 grains released after the decomposition of zircon were found in the same regions with white coloured Y_2O_3 particles where they were located predominantly surrounding of dark gray coloured MgO grains and rarely at MgO grain boundaries. It was observed that light gray coloured forsterite phases were mainly located between MgO grains and ZrO_2 + Y particles, where the concentrations of MgO and SiO_2 distributions were significantly intensive in those zones (Figs. 11 and 12). Furthermore, light gray coloured spinel phases overlapping MgO and Al_2O_3 distributions were in general situated in much broader areas that were outside of the zones where MgO grains and ZrO_2 + Y particles were present together.

M–S–(zircon + Y) containing materials during cooling after sintering create significant tensile stresses around additives due to the marked difference between the thermal expansion coefficients[36,38] (α) of MgO, spinel, zircon and Y_2O_3 ($\alpha_{MgO} = 13.6 \times 10^{-6}\,^{\circ}C^{-1}$, $\alpha_{Spinel} = 8.4 \times 10^{-6}\,^{\circ}C^{-1}$, $\alpha_{zircon} = 4.6 \times 10^{-6}\,^{\circ}C^{-1}$, $\alpha_{Y_2O_3} = 60.3 \times 10^{-6}\,^{\circ}C^{-1}$) and such stresses cause formation of interlinked microcracks.[14,15,33] It was observed that the microcracks forming in the structure are interlinked to each other and propagate for a short distance and are arrested or display deviation when coming across the Y_2O_3 grains found together with ZrO_2 released after the decomposition of zircon or when reaching the pores (Figs. 11 and 12). These identified microstructural factors are associated with the improvement occurring in the mechanical properties of zircon + Y added composite refractories.

R thermal stress parameter values used in determining high temperature performances of composite refractories are given in Fig. 13. *R* parameter is the maximum temperature difference allowed in the body under steady-state temperature flow in a solid with voids and pores and represents the minimum temperature difference required for the initiation of fracture, showing the resistance against the initiation of the crack in the material.[35] M–20%S and M–30%S composite refractories to which varied ratios of zircon + Y were added display a higher

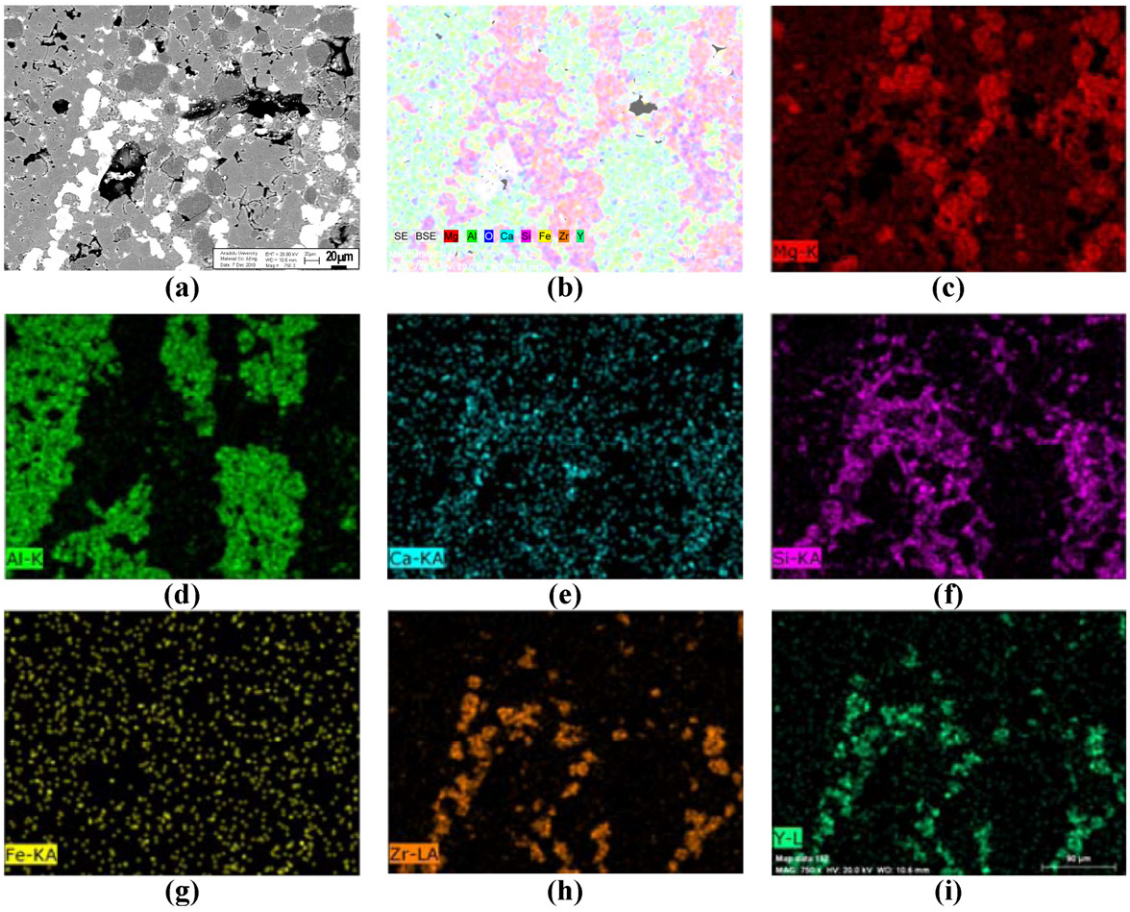

Fig. 11. Microstructural image of a composite refractory having M–30%S–20%(zircon + Y) composition [(a), (b)] and distribution of elements [(c) Mg, (d) Al, (e) Ca, (f) Si, (g) Fe, (h) Zr, (i) Y].

resistance against initiation of cracks with their higher R values compared to additive free M–S materials. The materials of M–5%S and M–10%S compositions produced by adding varied amounts of zircon + Y, on the other hand, have lower R values than M–S materials in general (except for 10%(zircon + Y) containing materials). It was observed that together with the amount of zircon + Y, spinel content was instrumental in the increase in R thermal stress parameter values. In composite refractories produced by adding zircon + Y additives to M–S; as a result of the formation of the forsterite (Mg_2SiO_4) phase when SiO_2 released due to decomposition of zircon into ZrO_2 and SiO_2 at approximately 1400 °C, goes into reaction with MgO, the bonding between MgO grains becomes stronger and in association with it, the resistance against crack initiation

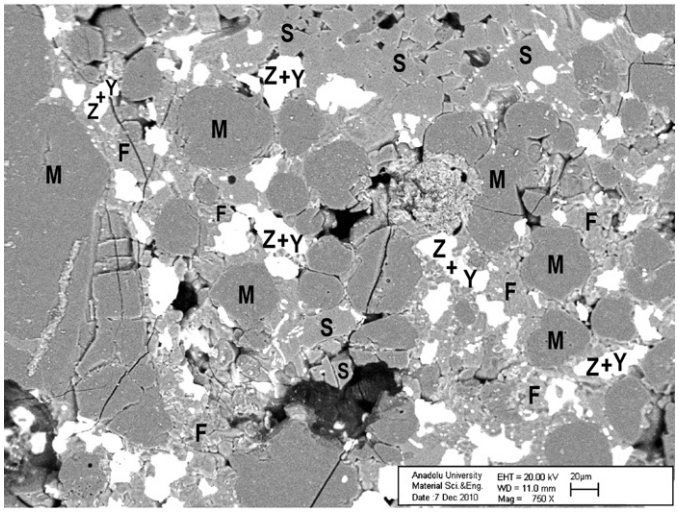

Fig. 12. Microstructural image of a material with composition of M–30%S–20%(zircon + Y) {dark gray: MgO (M), light gray: $MgAl_2O_4$ (S) and Mg_2SiO_4 (F), and white zones: ZrO_2 (Z) and Y_2O_3 (Y)}.

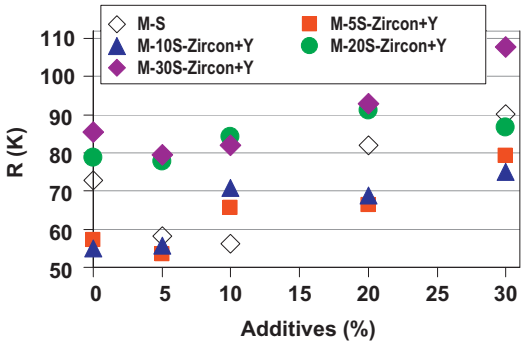

Fig. 13. R parameter as a function of additives {additives: (i) $MgAl_2O_4$ for M–S and (ii) $ZrSiO_4 + Y_2O_3$ for M–S–(zircon + Y)}.

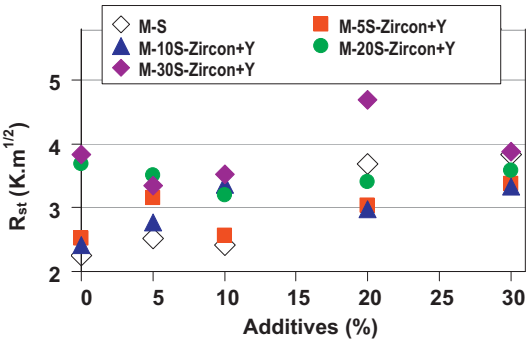

Fig. 14. R_{st} parameter as a function of additives {additives: (i) $MgAl_2O_4$ for M–S and (ii) $ZrSiO_4 + Y_2O_3$ for M–S–(zircon + Y)}.

increases. R values for M–S–(zircon + Y) compositions are high overall compared to M–S materials, increasing significantly in M–30%S–20%(zircon + Y) composition and reaching a maximum in M–30%S–30%(zircon + Y) composition. In comparison of the material containing M–30%S–30%(zircon + Y) with M–S compositions having maximum and minimum R values, which are (i) M–30%S and (ii) M–10%S, it was determined that higher resistance could be achieved against initiation of the crack at ratios reaching (i) 1.2-fold and (ii) 1.9-fold, respectively.

The R_{st} parameter represents the maximum temperature difference allowed required for propagation of long cracks under severe thermal stress conditions and is used in estimating the further weakening of the composite refractory and crack stability with the increase in the severity of thermal shock.[35] As shown in Fig. 14; while R_{st} thermal shock parameter values of M–S–(zircon + Y) composite refractories are in general higher than the R_{st} values of M–S materials up to10% additive incorporation, R_{st} values are typically lower than additive free M–S materials (apart from M–30%S–(zircon + Y) compositions) when 20% and 30% additives are introduced. The highest R_{st} parameter values were first attained in M–30%S–20%(zircon + Y) and subsequently in M–30%S–30%(zircon + Y) compositions (Fig. 14). In the comparisons of M–30%S–20%(zircon + Y) material with (i) M–30%S and (ii) M–10%S, which are M–S compositions having maximum and minimum R_{st} values, it was determined that higher resistance to thermal shocks could be achieved in ratios reaching (i) 1.2-fold and (ii) 2.0-fold, respectively.

R and R_{st} thermal stress/shock parameters can be used to characterise thermal shock damage. In industrial applications, crack propagation is much more difficult in refractory materials than the initiation of cracks.[39] The main concern is the resistance to crack propagation and to extension of damage caused by thermal shock, rather than resistance to crack initiation.[40–43] On the other hand, crack initiation resistance gives information about the ability of materials to withstand thermal shock, as defined by experience of a rapid temperature change without the initiation of a crack.[39] In this study; R and R_{st} parameters were calculated based on the mechanical properties, and thermal behaviour of materials was characterised and assessed on that basis. It was found that R and R_{st} parameters were consistent with each other, and the incorporation of zircon–Y_2O_3 into M–S compositions improved both crack initiation resistance and crack stability preventing the further weakening of composite refractory under severe thermal conditions. It was determined from the R and R_{st} parameter data that M–30%S–30%(zircon + Y) and M–30%S–20%(zircon + Y) composite refractories will display higher thermal stress resistance and thermal shock damage resistance compared to M–S materials and therefore, will have a longer service life at high temperatures in industrial use and this is consistent with the determined mechanical properties.

4. Conclusions

The basic parameters leading to the improvement of the mechanical properties and therefore the increase in thermal shock performance of M–S composite refractory materials with the addition of zircon + Y were determined as follows: (i) increase in bonding between MgO grains induced by the formation of the forsterite (Mg_2SiO_4) phase and consequently, the increase in resistance against crack initiation and propagation, (ii) propagation of the microcracks formed in the structure for a short distance by interlinking to each other, and (iii) arresting or deviation of microcracks when reaching pores or ZrO_2 particles released after decomposition of zircon, located together with Y_2O_3 particles, (iv) co-presence of both intergranular and transgranular types of fracture on fracture surfaces, and moreover with addition of zircon + Y, (v) the increase in density, and (vi) a significant reduction in MgO grain size.

With the addition of 30%(zircon + Y) to M–30%S, marked improvements were observed on the strength, modulus of elasticity, fracture toughness and fracture surface energy values by factors of 2.9, 2.7, 2.4 and 2.0, respectively. With the addition of (i) 30%(zircon + Y) and (ii) 20%(zircon + Y) to M–30%S, it was determined that composite refractory materials may display higher resistance to i) thermal stresses and initiation of cracks at ratios reaching 1.2- and 1.9-fold in R values and (ii) thermal shocks and propagation of cracks at ratios reaching 1.2- and 2.0-fold in R_{st} values, respectively. This is associated with the low loss of strength and high resistance against fracture, high thermal stress and high thermal shock damage resistance and therefore longer service life for M–S–(zircon + Y) composite refractories at high temperatures in industrial use.

Acknowledgements

This study was partly supported by Anadolu University and in part TUBITAK under Project No. 106M394 with partial support provided also by Konya Selcuklu Krom Magnezit Tugla Sanayi A.S. We would like to express our gratitude to A. Ozkaymak, R. Ozbasi, O. Bezirci, and all agency employees and personnel involved in this project for their support. We also thank the agencies and plant authorities for the supplied equipments and raw materials.

References

1. Cooper SC, Hodson PTA. Magnesia–magnesium aluminate spinel as a refractory. *Trans J Brit Ceram Soc* 1982;**81**:121–8.

2. Dal MR, Fabbri B, Fiori C. Industrial applications of refractories containing magnesium aluminate spinel. *Ind Ceram* 1988;**8**:121–6.
3. Bray DJ. Toxicity of chromium compounds formed in refractories. *Bull Am Ceram Soc* 1985;**64**:1012–6.
4. Tabbert W, Klischat HJ. Magnesia spinel bricks for the cement industry. In: *Beijing China Symposium*. 1992. p. 424–30.
5. Kuennecke M, Wieland K, Faizullah M. The correlation between burning zone linings and operation of cement rotary kilns – part 2. *World Cem* 1986:247–53.
6. Bartha P. Magnesia spinel bricks–properties production and use. In: Zhong X, editor. *Proc. Int. Symp. Refractories, Refractory Raw Materials and High Performance Refractory Products*. Hangzhou: Pergamon; 1989. p. 661–74.
7. Eusner GR, Hubble DH. Technology of spinel bonded periclase brick. *J Am Ceram Soc* 1960;**43**:292–6.
8. Evans RM. Magnesia–alumina spinel raw materials production and preparation. *Am Ceram Soc Bull* 1993;**72**:59–63.
9. Gonsalves GE, Duarte AK, Brant PORC. Magnesia–spinel brick for cement rotary kilns. *Am Ceram Soc Bull* 1993;**72**:49–54.
10. Carbone TJ. Characterization and refractory properties of magnesium aluminate spinel raw materials. *Interceram Spec Issue* 1985:91–4.
11. Bartha P. Using magnesia–spinel bricks to prevent the formation of rings in rotary cement kilns. *World Cem* 1990:98–100.
12. Ghosh A, Sarkar R, Mukherjee B, Das SK. Effect of spinel content on the properties of magnesia–spinel composite refractory. *J Eur Ceram Soc* 2004;**24**:2079–85.
13. Sarkar R, Tripathi HS, Ghosh A. Reaction sintering of different spinel compositions in the presence of Y_2O_3. *Mater Lett* 2004;**58**: 2186–91.
14. Aksel C, Riley FL. Magnesia–spinel ($MgAl_2O_4$) refractory ceramic composites. In: Low IM, editor. *Ceramic matrix composites: microstructure, properties and applications*. USA: Woodhead Publishing Limited and CRC Press LLC; 2006. p. 359–99.
15. Aksel C, Rand B, Riley FL, Warren PD. Mechanical properties of magnesia–spinel composites. *J Eur Ceram Soc* 2002;**22**:745–54.
16. Aksel C, Warren PD. Work of fracture and fracture surface energy of magnesia–spinel composites. *Compos Sci Technol* 2003;**63**: 1433–40.
17. Sahin B. Examination of mechanical properties of MgO–spinel composite refractories with the addition of zircon–Y_2O_3. MSc thesis, Anadolu University, Eskisehir, Turkey, 2008.
18. BS 7134, *Methods for determination of density and porosity*, British Standard Testing of Engineering Ceramics, Part 1, Section 1.2, 1989.
19. ASTM C1161-90. Standard test method for flexural strength of advanced ceramics at ambient temperature. In: *Annual book of ASTM standards, 15.01*. ASTM; 1991. pp. 327–33.
20. ASTM D790M-86. Standard test methods for flexural properties of unreinforced and reinforced plastics and electrical insulating materials. In: *Annual book of ASTM Standards, 08.01*. ASTM; 1988. pp. 290–8.
21. Larson DR, Coppola JA, Hasselman DPH. Fracture toughness and spalling behaviour of high-Al_2O_3 refractories. *J Am Ceram Soc* 1974;**57**: 417–21.
22. ASTM E399-90. Standard test method for plane–strain fracture toughness of metallic materials. In: *Annual book of ASTM standards, 03.01*. ASTM; 1991. pp. 485–515.
23. ASTM D5045-91. Standard Test Methods for plane–strain fracture toughness and strain energy release rate of plastic materials. In: *Annual book of ASTM standards, 08.03*. ASTM; 1991. pp. 728–36.
24. Brown WF, Srawley JE. Plane strain crack toughness testing of high strength metallic materials, ASTM Special Technical Publication, No. 410, 1967.
25. Griffith AA. The theory of rupture. In: Proceedings of the First International Congress for Applied Mechanics. 1924. p. 55-63.
26. Davidge RW, Tappin G. The effective surface energy of brittle materials. *J Mater Sci* 1967;**3**:165–73.
27. Griffith AA. The phenomena of rupture and flow in solids. *Philos Trans R Soc Lond* 1920;**A221**:163–98.
28. Sack RA. Extension of Griffith's theory of rupture to three dimensions. In: Proc Physical Soc. Vol.58, London; 1946. p. 729-36.
29. Davidge RW. Mechanical behaviour of ceramics. Cambridge: Cambridge University Press; 1979.
30. Morrell R. Handbook of properties of technical and engineering ceramics. Part 1. London: Her Majesty's Stationery Office; 1985.
31. Aksel C, Riley FL. Effect of particle size distribution of spinel on the mechanical properties and thermal shock performance of MgO–spinel composites. *J Eur Ceram Soc* 2003;**23**:3079–87.
32. Aksel C, Riley FL. Young's modulus measurements of magnesia–spinel composites using load–deflection curves, sonic modulus, strain gauges and Rayleigh waves. *J Eur Ceram Soc* 2003;**23**:3089–96.
33. Aksel C, Warren PD, Riley FL. Fracture behaviour of magnesia and magnesia–spinel composites before and after thermal shock. *J Eur Ceram Soc* 2004;**24**:2407–16.
34. Mendelson MI. Average grain size in polycrystalline ceramics. *J Am Ceram Soc* 1969;**52**:443–6.
35. Hasselman DPH. Thermal stress resistance parameters for brittle refractory ceramics: a compendium. *Am Ceram Soc Bull* 1970;**49**:1033–7.
36. Shackelford JF, Alexander W, Park JS, editors. *CRC materials science and engineering handbook*. Boca Raton, FL: CRC Press; 1994.
37. Burnett SJ. Properties of refractory materials. Harwell: UKAEA Research Group Report; 1969.
38. Hayaski H, Saitou T, Maruyama N, Inaba H, Kawamura K, Mori M. Thermal expansion coefficient of yttria stabilized zirconia for various yttria contents. *Solid State Ionics* 2005;**176**:613–9.
39. Bradt RC. Fracture testing of refractories, past present and future. In: Proc 2nd Int Conf on Refractories. Tokyo; 1987. p. 61-8.
40. Semler CE, Hawisher TH, Bradt RC. Thermal shock of alumina refractories: damage-resistance parameters and the ribbon test. *Am Ceram Soc Bull* 1981;**60**:724–9.
41. Semler CE, Bradt RC. Thermal shock damage of magnesite chrome refractories in the ribbon test. *Am Ceram Soc Bull* 1984;**63**:605–9.
42. Coppola JA, Bradt RC. Thermal shock damage in SiC. *J Am Ceram Soc* 1973;**56**:214–7.
43. Ainsworth JH, Herron RH. Thermal shock damage resistance of refractories. *J Am Ceram Soc* 1974;**53**:533–8.